21, rue d'Artois, F-75008 PARIS
http: //www.cigre.org

CIGRE US National Committee
2021 Grid of the Future Symposium

Real-Time Controller Hardware-in-the-Loop (RT CHIL) Analysis of Ground Fault Overvoltages (GFOVs) in Inverter-based Distributed Energy Resources (DERs)

P.M. ADHIKARI[1], L. VANFRETTI[1], M. RUPPERT[2], M. ROPP[3]
Rensselaer Polytechnic Institute[1], JEM Engineering[2], Northern Plains Power Technologies[3] USA

SUMMARY

Single-line-to-ground (SLG) faults can lead to a significant overvoltage on the unfaulted phases of a 3-phase system that is fed by a synchronous generator. In order to mitigate such ground-fault overvoltages (GFOV) certain effective grounding techniques are employed in the system. However, for systems fed by inverter based Distributed Energy Resources (DER) the GFOV phenomenon is not studied in detail. Moreover, whether or not conventional overvoltage mitigation techniques like effective grounding techniques are suitable for overvoltage mitigation for inverter based DERs, also needs significant exploration. In this paper a controller-hardware-in-the-loop (CHIL) setup was utilized to carry out experiments which investigate how the circuit configuration impacts the overvoltage for DERs under SLG and how conventional grounding techniques can be utilized to mitigate such overvoltages.

KEYWORDS: Controller-Hardware-in-the-Loop (CHIL), Typhoon HIL 604, Ground Fault Overvoltage, Real Time Simulation.

prottaymondaladhikari@gmail.com

I. INTRODUCTION:

A. Motivation:

It has been studied that about 80% of all the faults that occur in power systems are single line to ground (SLG) faults. It is also observed that SLG faults occurring on a system supplied by ungrounded synchronous generators can give rise to an overvoltage of upto 173%. To eliminate this overvoltage problem, IEEE std 62.92.2 proposed effective grounding techniques for synchronous generators. Additionally, IEEE std 62.92.3, 62.92.4, 62.92.5 discusses the grounding standards for generator auxiliaries, distribution systems, and transmission systems- respectively. However, the grounding requirement from distributed energy resources- specifically, inverter-based energy sources are not standardized and are not discussed in detail, yet. Thus, this work explores the grounding requirements for inverter based energy sources, under SLG faults. For this particular work, the PV-inverter was connected to a PV array (represented by a DC source), which makes this research very relevant in the context of massive increase in the renewable energy penetration in recent times.

B. Related Works:

The authors in [1] laid out the mathematical and experimental foundations on whether or not effective grounding is necessary for inverter based distributed energy systems. In that process, it extended the theory explored initially in [2]. Both these papers established the theoretical explanation behind the severe ground fault overvoltage (GFOV) typically seen in ungrounded 4 wire/3-phase distribution systems supplied by synchronous generators. For traditional generator-based systems, the severity of ground faults is discussed in [4] in the context of Romanian power grid. The results presented in [1] also include a simple sequence analysis to explain such overvoltage phenomena for inverter based DERs. It showed that mathematically, these overvoltages can be best formulized by a sudden increase in the negative sequence voltage. This hypothesis was also supported by a very detailed sequence analysis of similar inverter based distributed energy systems, performed by [3]. However, distribution systems featuring inverter based generation, when subjected to higher load, exhibit both ground-fault overvoltage (GFOV), and load rejection overvoltage(LROV). It is important to distinguish between these two phenomenons while experimenting on inverter based distributed energy systems subjected to higher loads. A comprehensive comparison between [5] and [6] reveals the distinct features of GFOV and LROV, and how to distinguish one from the other.

Usage of real-time-simulators in power and energy studies has been a subject of interest for a long time. Authors in [7] reported an extensive comparison between different real-time simulation platforms including eMEGAsim(Opal-RT), RTDS, HYPERSIM(Opal), dSPACE, VTB, xPC and Typhoon. [8] compared the software packages used in Opal-RT and Typhoon HIL real-time simulator-platforms. The research reported in [9], [10], [11] are very important in the context of using grid-connected PV inverters. This paper uses the same hardware and software platform reported in [9]-[11], hereinafter referred as the AIT SGC. This AIT SGC infrastructure was used to construct the system shown in Fig. 4. This architecture supports standard Modbus protocols, and is compliant to SunSpec specifications [12]. The inverter implementation followed a T-type topology which was reported in [15]-[17] and archived as a library element in [19]. The report in [18] illustrates a commercial implementation of this topology.

Contributions:

- Real-time modeling and CHIL implementation of a grid-connected inverter based system supporting a balanced resistive load.
- Designing a grounding transformer to mitigate the overvoltages in the said system, when put under an SLG condition. Investigations were also carried out to test how effective such mechanisms are in mitigating the overvoltage.
- Tests were performed from the load-side to analyze the effectiveness of the grounding transformers in inverter-based systems under different loading conditions.

II. THEORETICAL BACKGROUND:

There are two major components of the mathematical foundation of this research. Since, detailed analysis were beyond the scope of the main body of this paper, those analyses are presented in appendix. Appendix B reviews the mathematical background of the GFOV phenomenon for synchronous generators and inverters.

Appendix C explores the theoretical methodology for designing grounding transformers targeted for inverter based DERs.

III. EXPERIMENTAL SETUP:

This section focuses on (i) The circuit modeled to perform the analysis, and (ii) The real-time hardware and controller configuration utilized to perform the tests.

A. Modeling of the circuit:

The circuit under test consisted of a hard PV system (simplified as a DC source) connected to a T-type 3 phase inverter followed by a well-designed filter bank. This inverter converts the DC voltage into balanced 3 phase sinusoidal voltages. This 3-phase system is connected to a step up transformer which increases the voltage level from 480V to 13.2kV. This 13.2kV voltage level matches the voltage of the utility grid used in the system. This grid-connected PV system supports a 3 phase UPF load of 500 kW. Figure 4 represents the overall system that was simulated. The detailed specifications are summarized in Appendix A.

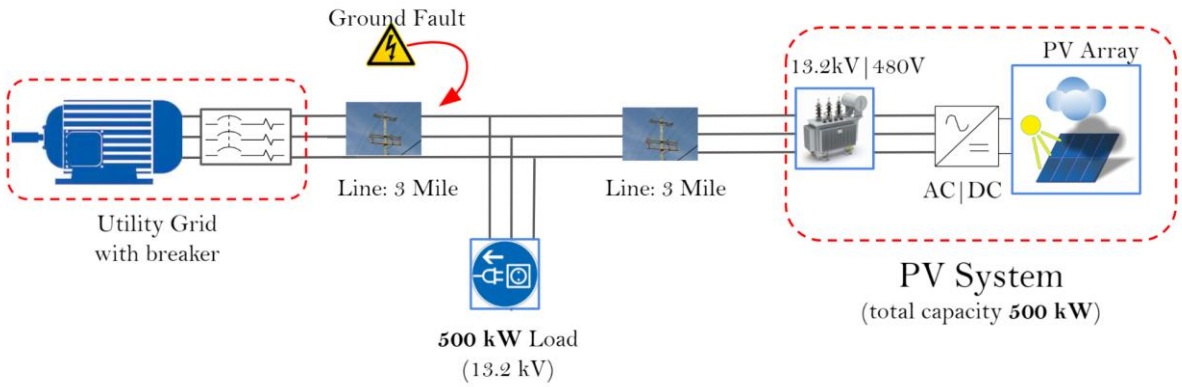

Fig 4: System under test: 500 kW load supported by grid connected PV-inverter

Because the system was designed for RT-simulation in Typhoon HIL 604, the modeling was done in Typhoon's proprietary software *Typhoon HIL Schematic.* The inverter was imported from Typhoon's internal *'converters'* library. This inverter incorporates a T-type topology for converting the DC input into 3-phase AC output which is archived in [19].

B. RT-Hardware/Software configuration for experimentation:

The RT-hardware used to simulate the inverter and the remainder of the circuit was Typhoon HIL 604. The inverter being simulated inside this simulator is controlled by the AIT Smart Grid Controller (ASGC) through an analog break-out board. The modeling of the circuit was accompanied with programmable breakers which were used to initialize the SLG fault and disconnect the utility grid from the rest of the system. In order to ensure that the switchings only happen near the zero-crossings of the currents in each phase, an additional parameter ε was introduced into the algorithm which defines the maximum acceptable duration of time before or after the current zero-crossings, when switchings are acceptable. The sequential process of introducing the SLG fault, and operating the utility-side breaker is summarized in Algorithm 1.

IV. EXPERIMENTAL RESULTS:

The key objective of this research was to demonstrate how the overvoltage varies with the variation of the load.

Algorithm 1: To run the experiment for GFOV in Typhoon environment

```
if ∠V_a −  θ < ε then
|    if  Faulter = 1 then
|    |
|    |   BKR_F = CLOSE
|    |   State= FLT
|    |   EXIT to next function
|    |
|    else
|      BKR_F = OPEN
|
else
       Continue Simulation

while State= FLT do
|
|      wait (35ms)
|      do in parallel
|          if
|           ∠I_a −  θ < ε then
|               BKR_A = OPEN
|          if
|          ∠I_b −  θ < ε then
|               BKR_B = OPEN
|          if
|          ∠I_c −  θ < ε then
|               BKR_C = OPEN
|
end
```

A. GFOV Simulation: Measurement Methodologies:

The IEEE standard [13] had reported that the maximum GFOV of an inverter-based system under SLG depends on the per unit negative sequence impedance of the inverter. The per unit negative sequence impedance of the inverter was estimated by measuring the negative sequence voltage and current across the output of the inverter. However, a precisely tuned capacitance bank was required to perform any sequence analysis on the system post-SLG, because without a capacitance bank, the frequency of the system starts rapidly varying as soon as the utility grid disconnects itself from the PV-inverter. Upon proper tuning of the capacitance bank, the inverter was able to sustain the frequency close to 60 Hz for a few cycles, before the inverter finally disconnects due to overfrequency.

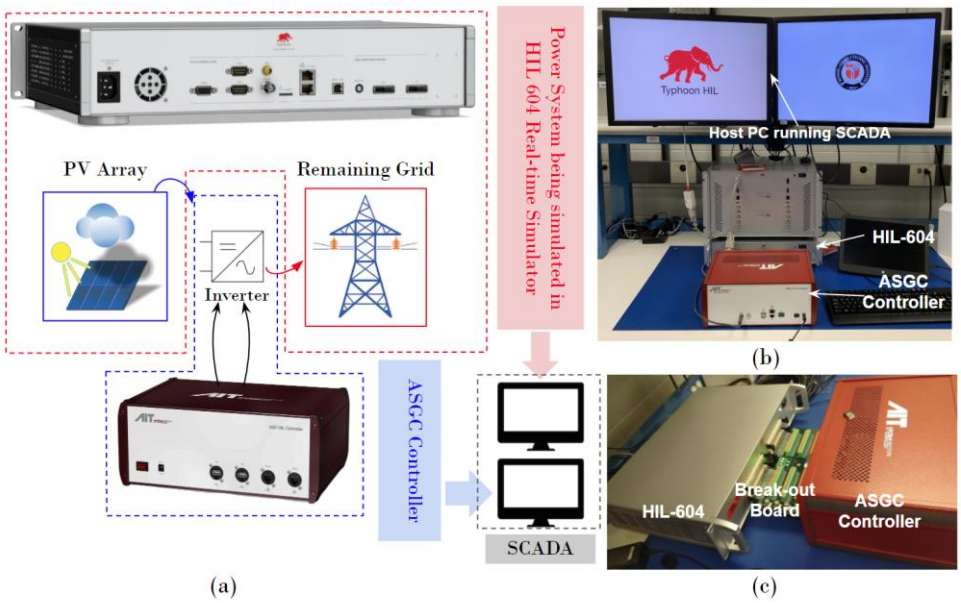

Fig 5: (a) The block-diagram representing the experimental hardware, (b) The experimental hardware, (c) The physical connection between the simulator and the controller.

The sequence components computations/measurements are to be performed while the utility has already disconnected, and the inverter is still supporting the 3-phase load close to 60Hz.

Figure 6 represents the switching sequence for introducing the SLG fault and disconnecting the utility source respectively. It can be seen that at t=0.5 sec, the SLG fault is introduced and around 0.53-0.55 sec the breakers disconnect the utility from the fault - leaving the inverter to feed the fault current by itself. The inverter provides fault current till 0.75 sec while it disconnects from the rest of the system. The GFOV should only be monitored and recorded through this duration. It can be seen in figure 7, that during this period of time, the frequency of the system gradually increases. It is also to be noted, that with the increase in frequency the positive and negative sequence components of the inverter current could no longer maintain a constant angle between themselves. In figure 8, it can be observed that due the frequency mismatch, this angle starts rapidly oscillating between -π and π after t=0.7 sec.Thus, it is impossible to apply any sequence analysis on its measurements after t=0.7 sec, and all the sequence analysis were performed on the data retrieved between t=0.6 to t=0.65 sec.

B. GFOV Simulation: Verifying the effect of GLR on GFOV:

It was observed that, while an SLG leads to a 73% overvoltage in synchronous generator-based systems, the overvoltage observed for inverter based systems under SLG were much less. In fact, when the inverter-generation matches the load, the overvoltage observed along the unfaulted phases was observed to be less than 10%. If the load is reduced (while keeping the power generation from the inverter constant),

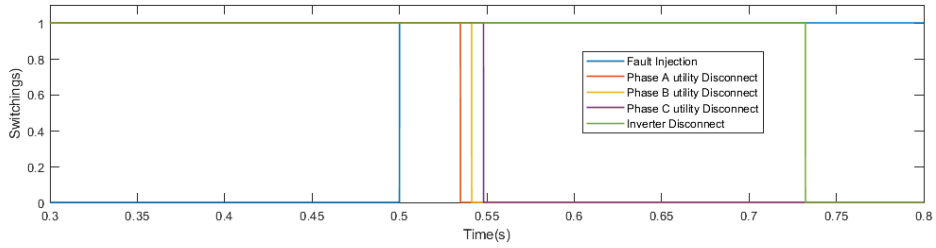

Fig 6: The Switching-sequence to replicate the experiment described as Algorithm 1

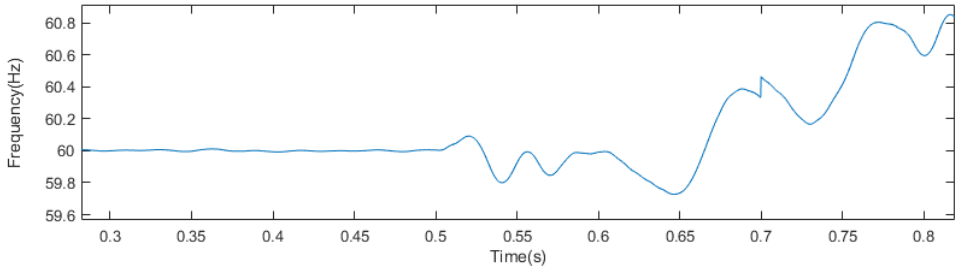

Fig 7: Frequency variation of the inverter based system after SLG

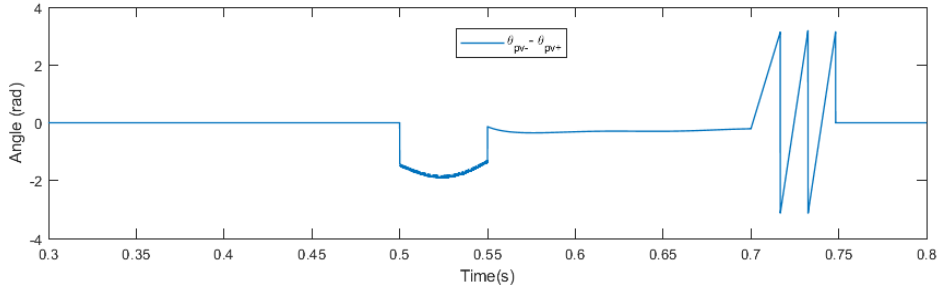

Fig 8: Variation of angle (between the positive and negative sequence components of inverter current) after SLG

the overvoltage is expected to increase according to the reports in IEEE standard 62.92.6. In fact, the maximum observed overvoltage increases in proportion to the generation to load ratio (GLR). This trend was reported in the IEEE std 92.62.6 [13] and verified with the Typhoon HIL based CHIL-RT simulation presented in this paper. A comparison between the data reported by [13] and the data obtained in the current research is presented in Figure 9.

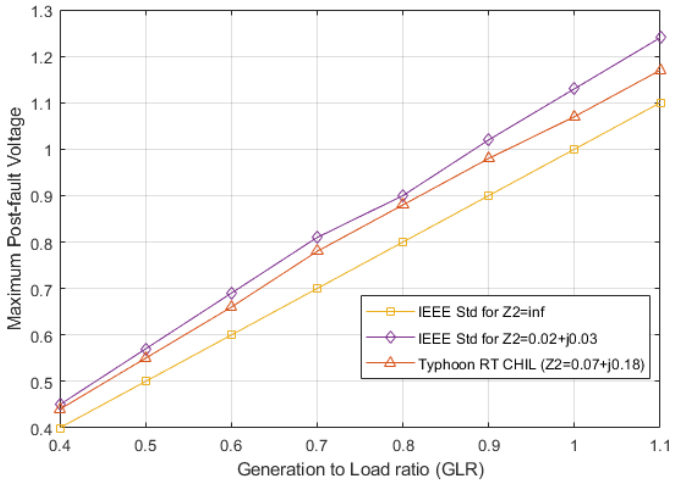

Fig 9: Variation of Maximum GFOV with varying Generation to load ratio: Comparison between the IEEE std and the results obtained from the current RT-CHIL experiments

The load was initially configured as a 500 kW 3 phase UPF load in wye connetion. However, in order to run different experiments, the load was varied from 333 kW to 1250 kW, while keeping the PV-inverter's output constant at 500 kW. This variation ensures that the generation to load ratio (GLR) is effectively varied from 0.4 (when the load is 1250 kw) to 1.5 (when the load is 333 kW). The variation of maximum overvoltage (GFOV) with the variation of GLR was reported in [14], [20] and analyzed in [22]. The observed GFOV v GLR trend was consistent with the trend reported in the IEEE standard 62.92.6 as presented in Fig. 9.

It is important to take note that, both the unfaulted phases are at the same level of overvoltage in this configuration, under SLG. This is illustrated in Figure 10. The magnitude of overvoltage for both the phases B and C are within 10%, when the generation matches the load.

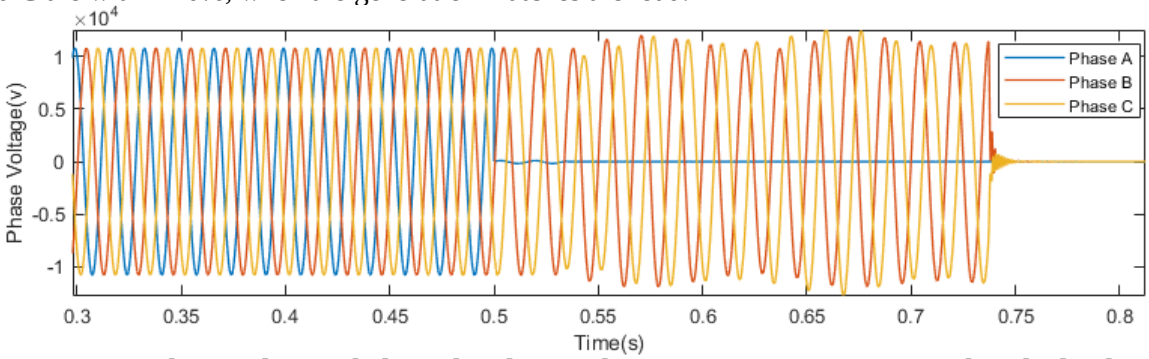

Fig 10: Voltages observed along the phases when inverter generation matches the load

C. GFOV Simulation: Introduction of Grounding Transformers:

Grounding transformers are efficient overvoltage mitigating infrastructure utilized in synchronous generator based 3 phase systems. However, their efficiency for mitigating overvoltages in inverter based DERs are relatively less explored.

As mentioned by the authors in [14] and illustrated in section appendix C, grounding transformers cannot mitigate the overvoltages appearing on **both** the unfaulted phases simultaneously. For validating this hypothesis, a grounding transformer is introduced in the simulation model. To emphasize its impact on the circuit, the connected grounding transformer was designed to be a significantly big one (i.e. 500 kW), which had a Yg-△ configuration. The modified system was then subjected to the same test that was illustrated in section IV.A. The overvoltages on the unfaulted phases were recorded and they are presented in figure 11. A closer observation at this figure reveals that, the ground fault overvoltage at unfaulted phase C was sufficiently mitigated by the grounding transformer, while the overvoltage on phase B remained unaffected by the action of the grounding transformer.

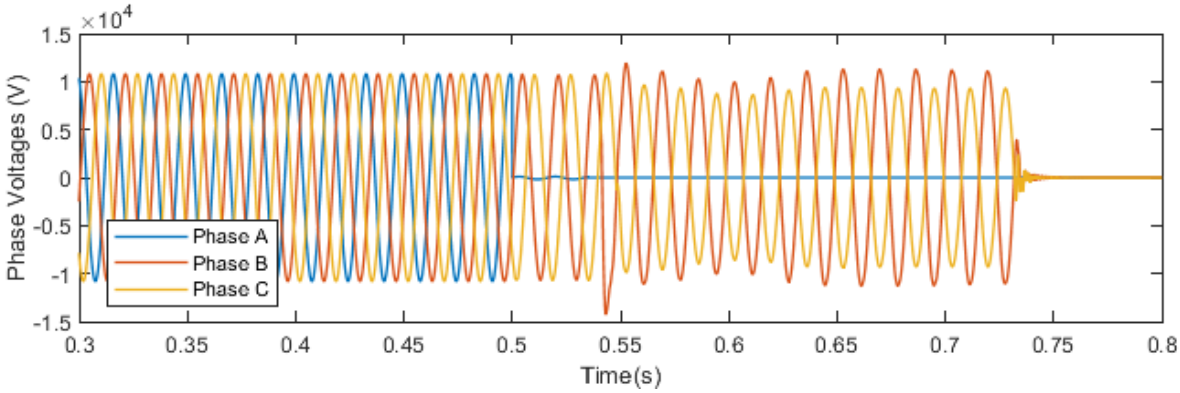

Fig 11: Voltages observed across the three phases when inverter generation matches the load and a Grounding transformer is connected to the system

This observation is analytically supported by the relationship presented in eqn (C5) in appendix C. It can be concluded from this relationship that the grounding impedance that can mitigate the overvoltage on phase B and the grounding impedance that would mitigate the overvoltage on phase C are different and it is only possible to mitigate the overvoltage on **one of the unfaulted phases** at a time. Figure 11 demonstrates that in this particular case, the grounding transformer mitigated the overvoltage on phase C successfully, while the overvoltage on phase B remained relatively unchanged.

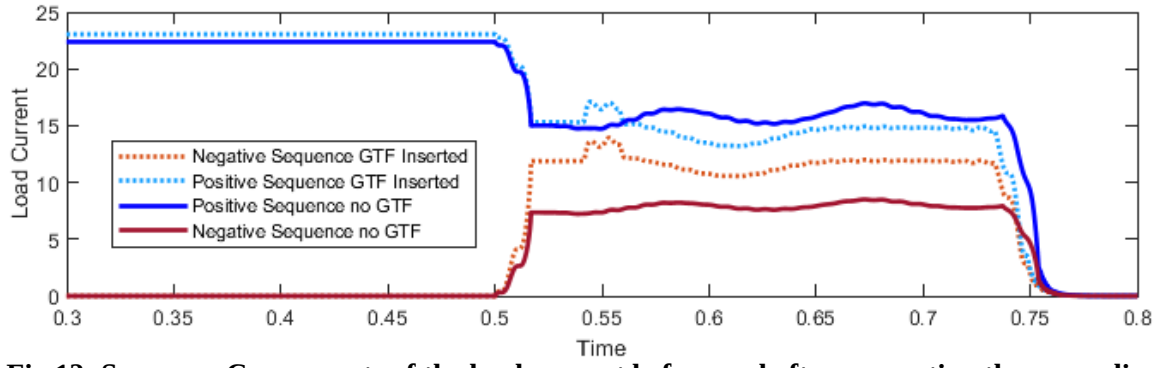

Fig 12: Sequence Components of the load current before and after connecting the grounding transformer

This observation can alternatively be explained by using sequence analysis. Introduction of the grounding transformer modifies the zero-sequence network, while keeping the negative sequence network as it was. In that process, it can mitigate ground-fault overvoltages. Figure 12 shows that, after the introduction of the grounding transformer in the current model, the negative sequence component of the load current under the SLG increases, in spite of the reduction of the zero sequence components of the post-SLG current. Because it cannot mitigate the increase in the negative sequence current it **cannot entirely** mitigate the overvoltage on the unfaulted phases. Table 1 illustrates that the introduction of the grounding transformer reduces the overvoltage on the unfaulted phases. It can also be concluded from the table that this improvement is minor (i.e. <5%). Since grounding transformers are expensive equipments and require expertise to operate and maintain, it is not advisable to incorporate them to mitigate ground fault overvoltages for inverter based DERs feeding only **wye** connected loads based on these experimental results.

D. GFOV Simulation: Introduction of Δ connected loads:

While section IV.C explores the utilization of grounding transformers for mitigating overvoltage in wye connected loads subjected to SLG, this section investigates whether Δ connected loads exhibit similar overvoltages and whether grounding transformers can be used to mitigate them. Thus, the existing wye connected load is re-configured to include considerable shares of Δ connected loads.

Table 1:

GLR	Over Voltage (Ground Fault No GTF)	Over Voltage (Ground Fault +GTF)
0.6	0.67	0.62 (improvement = 5%)
0.7	0.78	0.73 (improvement = 5%)
0.8	0.88	0.84 (improvement =4%)
0.9	0.990	0.935 (improvement = 5.5%)
1.0	1.0929	1.071 (improvement = 2.2%)
1.1	1.178	1.15 (improvement = 2.8%)
1.2	1.296	1.265 (improvement = 3%)

This updated system was simulated for observing GFOV both with and without the grounding transformer connected to the system. The observed overvoltages are summarized in table 2. It can be seen that the introduction of Δ connected loads into a system supported by inverter based DERs makes the system more vulnerable to ground fault overvoltages. However, it was interesting to observe that even though grounding transformers were not helpful in mitigating overvoltage in wye connected loads subjected to SLG, they can be effective in mitigating overvoltages in △ connected loads subjected to SLG.

Table 2:

Phase overvoltage on unfaulted phases when GLR=1.0	Y = 100%| △=0%	Y = 75%| △=25%	Y = 50%| △=50%	Y = 25%| △=75%
Overvoltage without GTF	1.089	1.19	1.32	1.48
Overvoltage with GTF	1.05	1.07	1.07	No good observations

This phenomenon can be explained well by simple sequence analysis. When Δ connected loads are introduced in the load, the zero-sequence circuit of the system gets modified. This leads to overvoltage in the zero-sequence circuit. This zero-sequence overvoltage translates into an overvoltage along the unfaulted phases. However, since the grounding transformer adjusts the zero-sequence circuit of the system, it manages to compensate for the overvoltage stemming from the zero-sequence voltage component. It is important to note that, for each test-case in table 2 (with increasing share of Δ connected load) the capacitance bank needs to be re-tuned, and this procedure is very time-consuming. This re-tuning ensures that the inverter manages to sustain the voltages for a few cycles after the utility disconnects. The comparison between Figures 13 and 14 shows that the introduction of a grounding transformer reduces the overvoltages in both phases B and C. However, a closer observation reveals that the voltage reduction is more in phase C than it is in phase B. This is similar to what was observed in a system without any Δ connected load and is supported theoretically by equation (C5). Overall, it was observed that the maximum overvoltage reduced from 19% to 7%, upon the utilization of the grounding transformer.

Similar observations were recorded when the share of Δ connected load is increased from 25% to 50%. Without the grounding transformer the overvoltage was observed to be around 32% (figures 15). The grounding transformer reduced this overvoltage from 32% to 7% (figures 16). Clearly, for systems with Δ connected loads the usage of grounding transformers leads to significant reduction in overvoltages.

Figures 17 and 18 demonstrate that, when the share of Δ connected load is increased to 75%, it was observed that the overvoltage under SLG condition was close to 50%. Upon the addition of the grounding transformer the inverter observes that `Vbn.max`, `Ib.max`, `Ic.max` flags are set from the ASGC controller side when the SLG fault is applied, and the breaker disconnects the utility from the rest of the system. These flags initiate the subroutine that disconnects the ASGC controller from the Typhoon HIL 604 simulator running

the inverter model. It was not possible to bypass this protective operation from the controller, and thus no overvoltage computation is reported for this case in table 2. The corresponding phase voltages can be observed in figure 18.

The objective of the current research is to investigate whether or not grounding transformers are suitable to mitigate the ground-fault overvoltages in inverter based DERs. The experimental results demonstrated in this section establishes that grounding transformers can be effective in mitigating ground-fault overvoltages in inverter based DERs **only** when there is some significant share of Δ connected load being provided by the DERs.

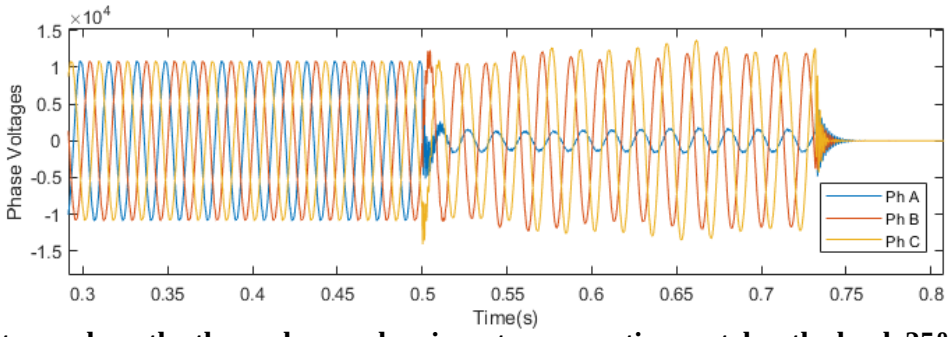

Fig 13: Voltages along the three phases when inverter generation matches the load, 25% of the load is Δ connected

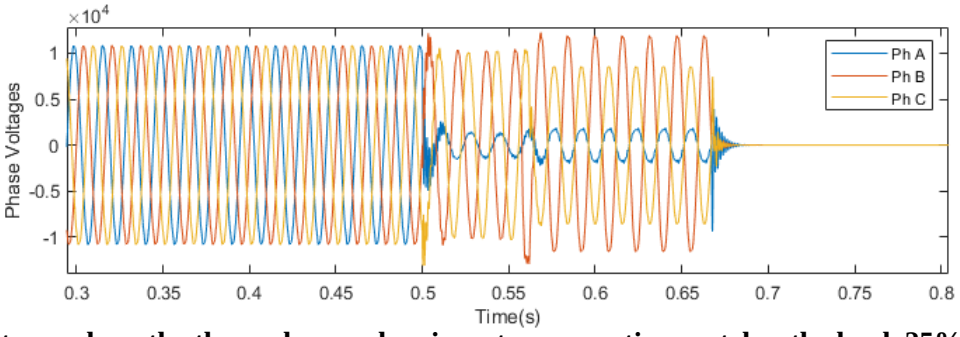

Fig 14: Voltages along the three phases when inverter generation matches the load, 25% of the load is Δ connected, a grounding transformer is connected to the system

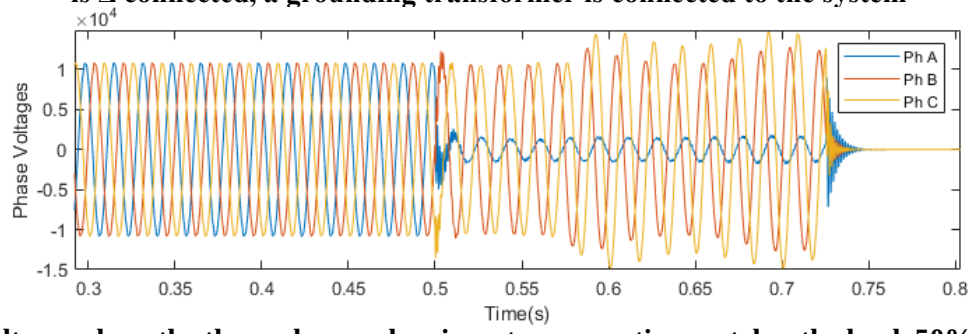

Fig 15: Voltages along the three phases when inverter generation matches the load, 50% of the load is Δ connected

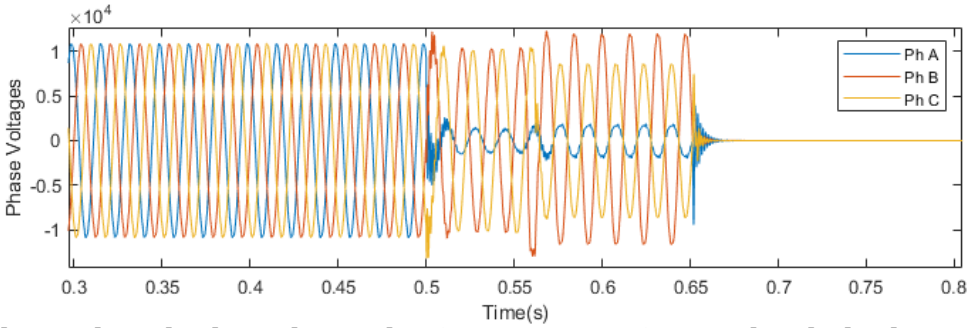

Fig 16: Voltages along the three phases when inverter generation matches the load, 50% of the load is Δ connected, a grounding transformer is connected to the system

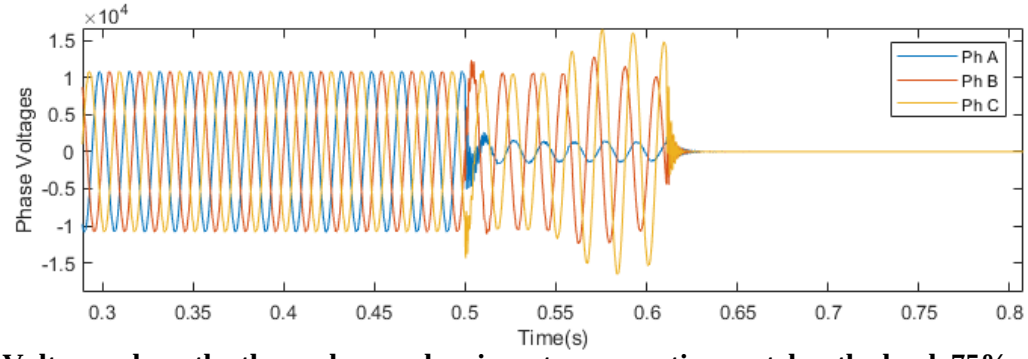

Fig 17: Voltages along the three phases when inverter generation matches the load, 75% of the load is Δ connected

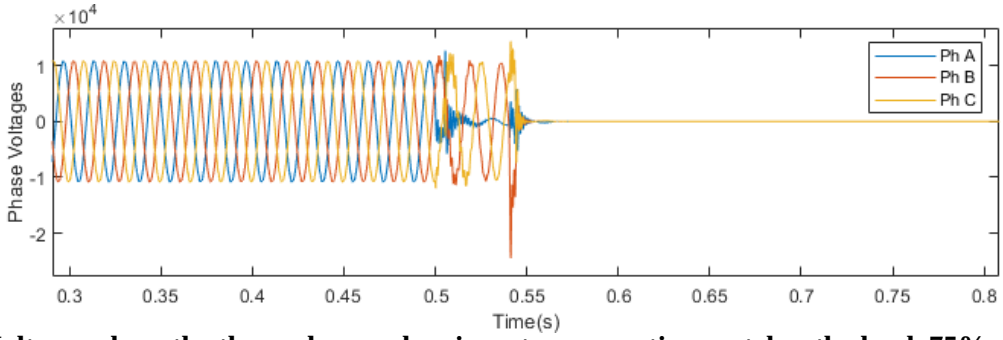

Fig 18: Voltages along the three phases when inverter generation matches the load, 75% of the load is Δ connected, a grounding transformer is connected to the system

V. CONCLUSIONS AND FUTURE WORKS:

This research explored whether ground fault overvoltages can be a concerning issue for inverter based DER supported systems, and whether traditional ground fault mitigation techniques like grounding transformers can be utilized to mitigate overvoltages in such systems. For experimentation, real-time simulation models were designed in Typhoon HIL 604 simulator, and the simulated inverter was externally controlled by the IEEE 1547 compliant ASGC controller. Through the course of the experiments, it was concluded that

- For Y connected loads supported by inverter based DERs, ground fault overvoltages are much less severe than they are for Y connected systems supported by synchronous generators.
- For Y connected loads, the small overvoltages observed during the SLG fault, cannot be efficiently eradicated on both unfaulted phases by introducing grounding transformers in the simulation model.
- When Δ connected loads are added to the system, the ground-fault overvoltage becomes more prominent.
- With DER-supported systems (with some share of Δ connected loads) exhibiting ground fault overvoltage, grounding transformers may provide an efficient technique to reduce the overvoltage significantly.

In terms of future work, experiments need to be performed with actual inverter hardware in the system instead of simulating the inverter inside the real-time simulator. Such experiments were beyond the scope of the current work. It needs to be noted that current research did not focus on inverter based DERs supporting non-UPF loads. Additionally, inverter modeling guidelines should be formalized based on these experiments, which was not reported in this paper.

ACKNOWLEDGEMENTS:

The authors wish to thank *Austrian Institute of Technology* for their inputs on this project and also like to acknowledge the support of *New York State Energy Research and Development Authority (NYSERDA)* for their sponsorship of the project. NYSERDA has not reviewed the information contained herein and the opinions expressed in this paper do not necessarily reflect those of NYSERDA or of the state of New York.

BIBLIOGRAPHY

[1] M. Ropp et al., "Ground Fault Overvoltage With Inverter-Interfaced Distributed Energy Resources," in IEEE Transactions on Power Delivery, vol. 32, no. 2, pp. 890-899, April 2017.

[2] P. Barker, "Overvoltage considerations in applying distributed resources on power systems," IEEE Power Engineering Society Summer Meeting,, Chicago, IL, USA, 2002, pp. 109-114 vol.1.

[3] W. Cao, Y. Ma, X. Zhang and F. Wang, "Sequence impedance measurement of three-phase inverters using a parallel structure," 2015 IEEE Applied Power Electronics Conference and Exposition (APEC), Charlotte, NC, 2015, pp. 3031-3038.

[4] A. Cerretti, F. M. Gatta, A. Geri, S. Lauria, M. Maccioni and G. Valtorta, "Temporary overvoltages due to ground faults in MV networks," 2009 IEEE Bucharest PowerTech, Bucharest, 2009, pp. 1-8.

[5] A. Nelson, A. Hoke, S. Chakraborty, J. Chebahtah, T. Wang, and B. Zimmerly, "Inverter Load Rejection Over-Voltage Testing ".

[6] Andy Hoke, Austin Nelson, Sudipta Chakraborty,Justin Chebahtah, Trudie Wang, Michael McCarty, "Inverter Ground Fault Overvoltage Testing "

[7] M. D. Omar Faruque et al., "Real-Time Simulation Technologies for Power Systems Design, Testing, and Analysis," in IEEE Power and Energy Technology Systems Journal, vol. 2, no. 2, pp. 63-73, June 2015.

[8] B. Azimian, P. M. Adhikari, L. Vanfretti and H. Hooshyar, "Cross-Platform Comparison of Standard Power System Components used in Real Time Simulation," 2019 7th Workshop on Modeling and Simulation of Cyber-Physical Energy Systems (MSCPES), Montreal, QC, Canada, 2019, pp. 1-6.

[9] P. Jonke et al., "Integrated rapid prototyping of distributed energy resources in a real-time validation environment," 2016 IEEE 25th International Symposium on Industrial Electronics (ISIE), Santa Clara, CA, 2016, pp. 714-719.

[10] B. Lundstrom, S. Chakraborty, G. Lauss, R. Bründlinger and R. Conklin, "Evaluation of system-integrated smart grid devices using software- and hardware-in-the-loop," 2016 IEEE Power & Energy Society Innovative Smart Grid Technologies Conference (ISGT), Minneapolis, MN, 2016, pp. 1-5.

[11] Roland Bründlinger, Ron Ablinger, Zoran Miletic AIT Smart Grid Converter(SGC) Controller featuring SunSpec protocol support utilizing Hardware-in-the-Loop (HIL) technology Available at:https://sunspec.org/wp-content/uploads/2016/09/AITSunSpecSmartGrid InverterControllerReferenceDesignwithSunSpecSVPsupportBrundlinger-final-160912.pdf

[12] Official Sunspec Specifications and Models. Available at: http://sunspec.org/interoperability-specifications/

[13] IEEE PC62.92.4 - Guide for the Application of Neutral Grounding in Electrical Utility Systems--Part IV: Distribution, Available at: https://standards.ieee.org/project/C62_92_4.html

[14] M. Ropp, Y. Cui, M. Kahrobaee, D. Schutz and C. Mouw, "On the Sizing and Benefits of Grounding Transformers with Distribution-Connected Inverters," 2018 IEEE/PES Transmission and Distribution Conference and Exposition (T&D), Denver, CO, USA, 2018, pp. 1-5, doi: 10.1109/TDC.2018.8440448.

[15] Z. Batool, S. Biricik, H. Komurcugil, T. Ngo and T. V. Vu, "Photovoltaic Supplied T-Type Three- Phase Inverter with Harmonic Current Compensation Capability," 2019 2nd International Conference on

Smart Grid and Renewable Energy (SGRE), 2019, pp. 1-5, doi: 10.1109/SGRE46976.2019.9020673.

[16] M. Aly, E. M. Ahmed, S. Kouro and M. Shoyama, "Capacitor Voltage Ripple Reduction Modulation Method for String Photovoltaic Inverters," *2019 21st International Middle East Power Systems Conference (MEPCON)*, 2019, pp. 852-857, doi: 10.1109/MEPCON47431.2019.9008065.

[17] V. Fernão Pires, D. Foito and D. M. Sousa, "Conversion structure based on a dual T-type three-level inverter for grid connected photovoltaic applications," *2014 IEEE 5th International Symposium on Power Electronics for Distributed Generation Systems (PEDG)*, 2014, pp. 1-7, doi: 10.1109/PEDG.2014.6878685.

[18] Texas Instruments' 3 Phase T-type string inverters. Available at: https://www.ti.com/solution/string-inverter?variantid=23181&subsystemid=23675

[19] Three-phase three-level T-type inverter/rectifier by Typhoon. Available at: https://www.typhoon-hil.com/documentation/typhoon-hil-software-manual/References/three-phase_three-level_t-type_inverter_rectifier.html

[20] IEEE Std C62.92.6™-2017: IEEE Guide for Application of Neutral Grounding in Electrical Utility Systems, PartVI—Systems Supplied by Current-Regulated Sources

[21] Prottay M. Adhikari, Luigi Vanfretti, Anja Banjac, Roland Br¨undlinger, Michael Ruppert, Michael Ropp, "Controller-Hardware-in-the-Loop Investigation of Ground Fault Overvoltage Phenomenon in Grid-Connected PV Inverters" submitted at *IEEE transaction on Power Delivery.*

APPENDIX A

Table A1: Circuit Specification of the simulated model

Component	Specification
Utility Source	Line-to-line voltage=13.2 kV 3 phase Short Circuit MVA= 180 X/R ratio = 8 Line construction= 336AA (phase), 3/o (Neutral)
Distribution Feeder	Z1=0.278+j0.682 Z0=0.757+j1.9532 Distance from PV source to load= 3 mile Distance from load to breaker= 3 mile
Distribution Transformer	3 phase, 480V/13.2kV kVA=500, Z=5%, X/R=10 Configuration Yg-Yg
PV System	500 kW, 0 kVAR
Load	Constant Power, Three-phase Original configuration: Phase to ground (Y) Compensating Capacitance (untuned) = 29.5 kVAR

APPENDIX B

GFOV Phenomenon:

The phase-to-ground voltages during unfaulted condition of the ungrounded synchronous generator as shown in Fig. 2. are given by

$$E_a = E\angle 0^o, E_b = E\angle 240^o, E_c = E\angle 120^o$$

Thus, in normal conditions $V_N = 0$. But, in faulted condition (phase C in the figure) the terminal voltage of phase C becomes 0. In this condition, on the load-side the voltage along phase C, V_{cn} goes to 0, as both ends of this phase are now effectively connected to the ground. In this situation, if KVL is applied along the loop comprising the B and C phases (the red dotted line in Fig. 2) the following expression is derived

$$E_b - V_{bn} - E_c = 0; \Rightarrow V_{bn} = E\angle 240^o - E\angle 120^o = \sqrt{3}E\angle 270^o$$

Similarly, applying KVL through phases A and C (blue dotted line in Fig. 2.) the load-side voltage on phase A, will be expressed as

$$E_a - V_{an} - E_c = 0; \Rightarrow V_{an} = E\angle 0^o - E\angle 120^o = \sqrt{3}E\angle 330^o$$

Clearly, from the above expressions it can be seen that the 73% ground-fault overvoltage is mathematically expected, and requires proper standardized measures to mitigate it.

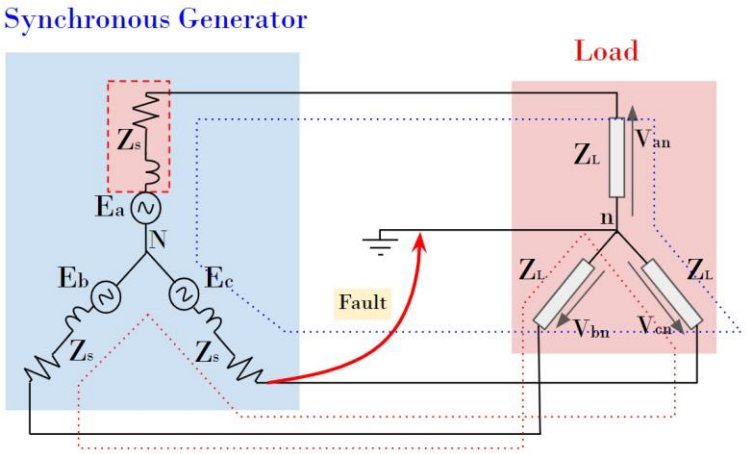

Fig B1: Single-line-ground (SLG) fault on Synchronous generator based 3-phase system

In Fig. 3 a similar setup is shown with a three-phase inverter instead of the synchronous generator. In the previous case when the fault strikes, the phase C of the synchronous generator was still maintaining E_c because the excitation system was still present and running. However, in Fig.3, the inverter does not have an internal voltage source, and it is modeled as a current source. Thus the voltage between terminal C and neutral N, is not maintained. In this situation, the voltages of the unfaulted phases on the load side will be

$$V_{an} = I_a \times Z_a, V_{bn} = I_b \times Z_b \text{ (B1)}$$

It can be seen that, in case the current provided by the inverter remains constant, there should not be any significant overvoltages on the unfaulted phases. However, in reality, the inverter is expected to increase its power output of each two unfaulted phases to 150%, to maintain the overall power output at the pre-fault level.

$$P = 1.5 \times P_{old} = \frac{V_{an}^2}{Z} \Rightarrow 1.5 \times \frac{V_{old}^2}{Z} = \frac{V_{an}^2}{Z}$$
$$\Rightarrow 1.5 \times V_{old}^2 = V_{an}^2 \Rightarrow V_{an} = 1.22 \times V_{old} \text{ (B2)}$$

Theoretically, if the inverter is to supply the same amount of load even after the fault, the load side voltage on the unfaulted phases can rise up to 22%. This value clearly, is much lower than the value (73%) derived in the case of synchronous generators.

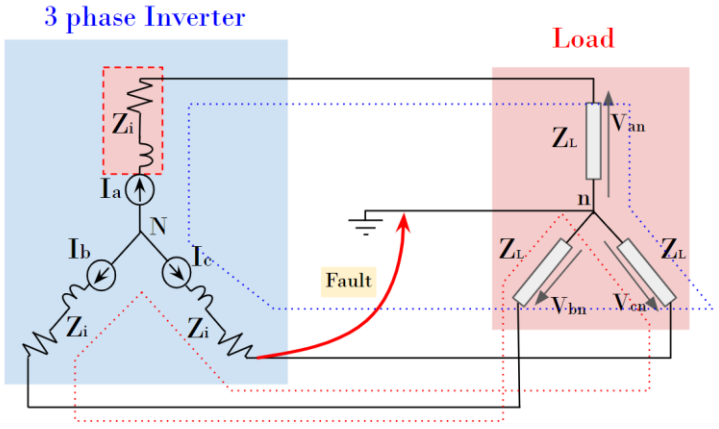

Fig B2: Single-line-ground (SLG) fault on inverter based 3-phase system

APPENDIX C:

Design of grounding transformer for inverters:

Figure 3 demonstrates the sequence diagrams of a system fed by an inverter based DER with (b) and without (a) the grounding transformer. It can be seen that the grounding transformer modifies the zero sequence network of the system. The representative circuit can be further simplified for a balanced Yg connected system by putting $Z_{load_0} = Z_{load-} = Z_{load+} = Z_L$

For the system in Fig. 3(b), the equivalent combined series impedance of the negative and zero sequence networks would be given as,

$$Z_{0-} = \frac{Z_L Z_{GTF}}{Z_L + Z_{GTF}} + Z_L = \frac{Z_L^2 + 2Z_L Z_{GTF}}{Z_L + Z_{GTF}} \text{(C1)}$$

Where Z_L is the load impedance and Z_{GTF} is the impedance of the grounding transformer used in the system. Applying the current division rule, it can be obtained that the current through the positive sequence network can be expressed as

$$I_+ = \frac{Z_L + Z_{GTF}}{2Z_L + 3Z_{GTF}} I_{PV}. \text{ (C2)}$$

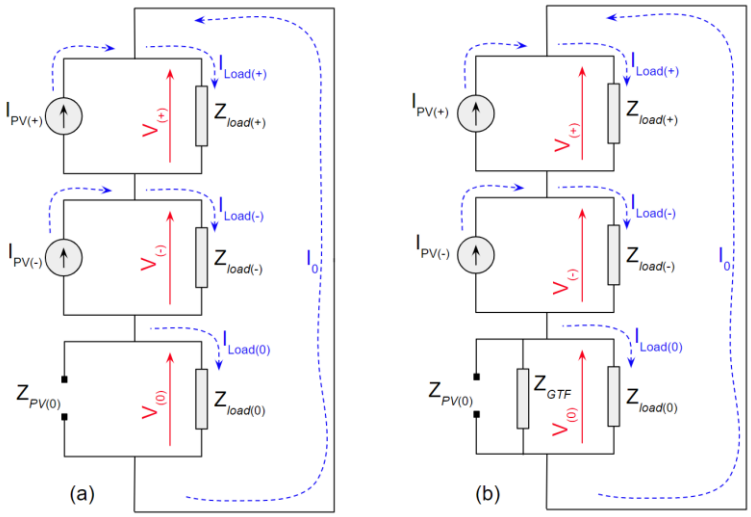

Fig A3: Sequence Diagram for Inverter based system under SLG with/without Grounding Transformer

Similarly, the negative and zero sequence currents will be equal to one another and they can be expressed as

$$I_{-0} = \frac{Z_L + 2Z_{GTF}}{2Z_L + 3Z_{GTF}} I_{PV} \text{(C3)}$$

These expressions assume that I_{PV} is the fault current after the SLG fault. Using these expressions for currents, the sequence components of the three phase voltages are calculated as

$$V_0 = -\frac{Z_{GTF}}{2Z_L + 3Z_{GTF}} I_{PV} Z_L \,,\; V_+ = \frac{Z_L + 2Z_{GTF}}{2Z_L + 3Z_{GTF}} I_{PV} Z_L, V_- = -\frac{Z_L + Z_{GTF}}{2Z_L + 3Z_{GTF}} I_{PV} Z_L \text{ (C4)}$$

From these expressions, the phase voltages of the unfaulted B and C phases can be calculated as

$$V_b = \frac{I_{PV} Z_L}{2Z_L + 3Z_{GTF}} [2a^2 Z_L + 3a^2 Z_{GTF} + Z_L], V_c = \frac{I_{PV} Z_L}{2Z_L + 3Z_{GTF}} [2aZ_L + 3aZ_{GTF} + Z_L] \text{ (C5)}$$

It is crucial to observe that the expressions for V_b and V_c are different, and there is no single value of Z_{GTF} which can minimize both their magnitudes at the same time. This analysis was supported by the analysis reported by the authors in [14] and is further validated through experimentation in section IV.